DISPERSION ASPECTS OF PM_{10} FROM POINT SOURCES IN A COMPLEX TERRAIN AREA WITH A MICROSCALE AND A MESOSCALE MODEL DURING AN EPISODE CASE

Vasileios N. Matthaios[1], Athanasios G. Triantafyllou[1] and Lakhdar Aidaoui[2]

[1]Laboratory of Atmospheric Pollution and Environmental Physics, Department of Environmental Engineering, Technological Education Institution (TEI) of Western Macedonia, 50100 Kozani, Greece

[2]Laboratoire de Développement en Mécanique et Matériaux, University of Djelfa, PB 3117, Djelfa, Algeria.

Presented at the 17th International Symposium on Environmental Pollution and its Impact on Life in the Mediterranean Region (MESAEP), September28 - October 01, 2013, Istanbul, Turkey

ABSTRACT

A simulation from three stacks of a power plant factory in a complex terrain, is attempted for the days of 2/12 and 3/12/11 where the most aggravating conditions were observed. For this simulation a mesoscale prognostic meteorological and air pollution model, The Air Pollution Model (TAPM), and a microscale computational fluid dynamics model (ANSYS-CFX) were used, configured and run for the two aforementioned days. Both models calculate the entrapment of PM_{10} during the afternoon and late morning hours of the simulation, while the development of a shallow convective atmospheric boundary layer, during the noon hours and the creation of a height inversion, leads to relatively high ground concentrations. Statistics performance of ANSYS and TAPM showed good correlation 0.94, 0.80 and 0.96 for the three cases that the numerical model was used.

KEYWORDS:
ANSYS and TAPM, Episode, Microscale modeling, Mesoscale modeling, Complex Terrain, Convective boundary layer.

1. INTRODUCTION

Modeling and its applicability in environmental situations is considered to be a tool that is developed and applied from scientists and researchers in order to simulate real cases. More specifically, simulations of area, line and point sources, as well as analysis of extreme meteorological conditions with model implementation such as cyclones, dynes, inversions and complex terrain, are of high interest in the research community [1-5]. Moreover, modeling is related to impact assessment studies to represent phenomena from a micro scale to a high scale. Another advantage of modeling is that weather forecast is directly linked with pollutants concentrations, helping the modeler to prevent or predict pollution episodes [6-8]. Many computer-based models have been developed for predicting pollutant dispersion. However, despite the fact that, computers are evolving rapidly to solve more complex algorithms, most of the models are based on empirical formulae. Therefore it is important that numerical complex models which are based on Navier –Stokes equations to be provided with many input parameters and with the knowledge of real atmospheric boundary layer in a mesoscale level, that is going to be simulated [2, 9].

Several reports have been made to simulate dispersion from factory stacks (point sources) [10-12, 16-18]. A study considering the basins' power plants used a coupled atmospheric mesoscale model and a Lagrangian dispersion model to investigate the pollutants transport conditions, plume impingement cases, fumigations and the atmospheric conditions that favor pollutant concentration [10]. Another study, concerning computational fluid dynamics from stacks dispersion, has been made by using computational fluid dynamics model ANSYS- CFX, comparing it with different models-approaches for 100m, in order to investigate the dispersion of pollutants from a multiflue calcination stack [11].

In this study, a mesoscale prognostic meteorological and air pollution model (TAPM) and a microscale computational fluid dynamics model (ANSYS-CFX) were configured for a complex terrain area in order to investigate the mechanism that favors the accumulation of pollutants, as well as the dispersion conditions in the lower parts of the atmosphere during an episode case. At the time that the episode was observed, high pressures were covering southeastern area of Europe, resulting to the degradation of the

* Corresponding author

surface wind field and to the absence of significant upward motions. The above synoptic conditions contributed to the gradual increase of relatively high pollutants concentrations, which were measured during that period [19]. The concentrations of PM_{10} during the two days of the simulation were four times higher than the average monthly value. For this occasion, the lowest in height power plant stacks was chosen (see Table 1.); with the intension of investigating the dispersion mechanism that might lead to relatively high ground concentrations in the area. It should be noted that the stack height from the other power plants in the area are 200m, and therefore, model simulations were carried out only for the particular power plant. More specifically, the simulations include a TAPM model configuration covering the area of approximately 30x30 km^2 to the inner grid of the simulation; with data assimilation in winds from 10 meteorological stations in the area of interest for meteorology [16]. While, as far as pollution is concerned in the same domain, the area that was covered is 13.5x13.5 km^2. In parallel, an ANSYS-CFX model configuration including the industrial sources (three stacks' emissions) in their real position has been built, in order to simulate the PM_{10} dispersion in space, in a cubic domain of 500m in each direction.

2. MATERIALS AND METHODS

2.1 Study area

The area of interest for the simulation is the basin in the axis of the Greek cities of Kozani and Ptolemais. This is a heavily industrialized area, which can be characterized as a broad, relatively flat bottomed basin surrounded by tall mountains, with height from 600 to more than 1500m above mean sea level. It is approximately 50 km in length and the width ranges from 10 to 25 km. The basin axis has a northwest to southeast direction. Furthermore, south from the valley the artificial lake of Polifitos is located. This lake together with the four natural lakes of Petron, Vegoritida, Ximaditida and Zazari in the north and northwest location, characterize the topography as fairly complex. In addition to that, four lignite power stations in the basin are operated by the Greek Public Power Corporation, with lignite mined in the nearby open pit mines. The climate of the area is continental Mediterranean with low temperatures during winter and high ones during summer, signifying rather strong temperature inversions during the whole year [5]. Figure 1 shows the topography of the region, including the two major cities, the power stations as the only source for the simulation, as well as the peripheral meteorological stations.

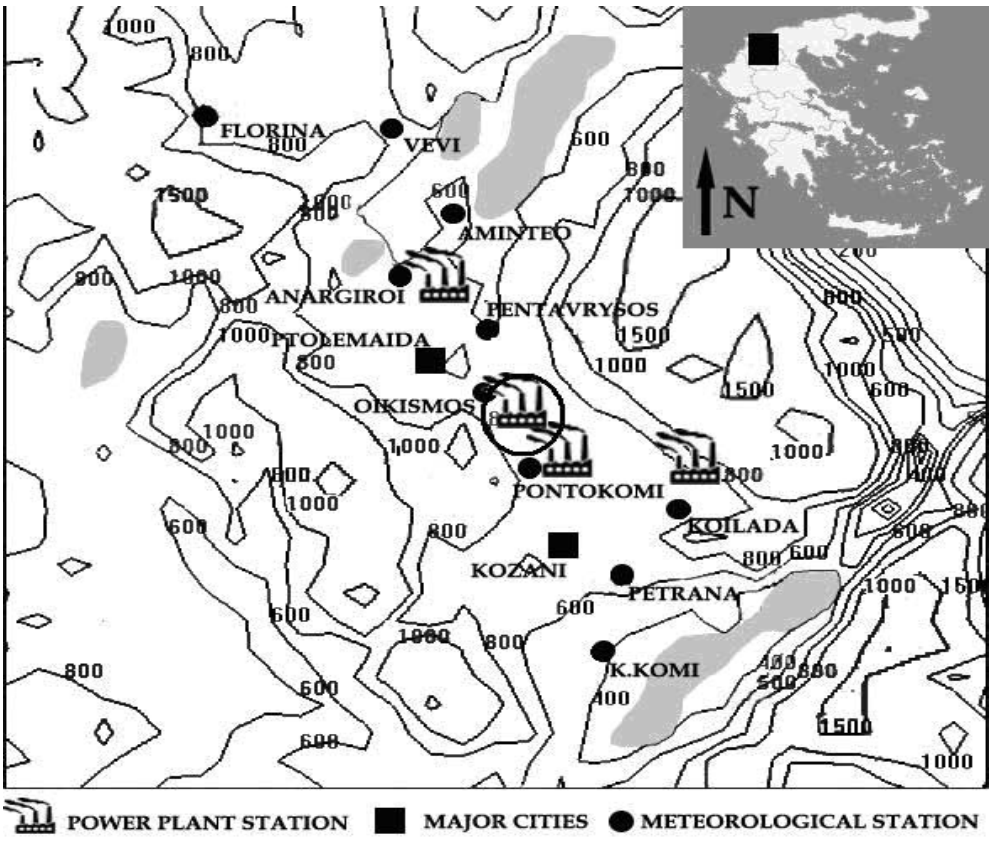

FIGURE 1 - Topography of Western Macedonia, including the peripheral stations for data assimilation and the power plants. In circle is the Power Plant station that was simulated. Elevations are in meters.

2.2 The dispersion model TAPM

TAPM is a nestable, prognostic meteorological and air pollution model that solves fundamental fluid dynamics and scalar transport equations to predict meteorology and pollutant concentration for a range of pollutants important for air pollution applications. For computational efficiency, it includes a nested approach for meteorology and air pollution, with the pollution grids optionally being able to be configured for a sub-region and/or at finer grid spacing than the meteorological grid, which allows a user to zoom-in to a local region of interest quite rapidly. TAPM includes chemistry and deposition modes, where specific pollutants and their interaction with each other are represented. Eulerian and Langragian modules also exist as an option to the user, for a more accurate simulation. In addition, it includes parameterizations for cloud/ rain micro-physical processes, turbulence closure, urban canopy, soil and radiative fluxes. TAPM is also able to dynamically downscale 1º resolution National Centre for Environmental Prediction (NCEP) Global Forecasting System (GFS) analyses to local –scales for environmental applications [13-16].

More specifically, TAPM configuration characteristics that were chosen for this particular occasion are four nested grid domains for meteorology and pollution, covering 25 vertical model levels and 30x30 horizontal grid points. The center stack of the three was considered to be the center of the simulation (0,0,0), with coordinates to be obtained from Universal Transverse Mercator. In detail, the TAPM simulation grids are as follows:

- Outer grid of the simulation spacing 30x30 km^2 (7.5x7.5km^2 for pollution).
- Second grid of the simulation spacing 10x10 km^2 (2.5x2.5 km^2 for pollution).
- Third grid of the simulation spacing 3x3 km^2 (0.75x0.75km^2 for pollution).
- Inner grid of the simulation spacing 1x1km^2 (0.25 x0.25km^2 for pollution).

Data assimilation in winds from 10 regional stations shown in Figure 1 was included for meteorology while, as far as pollution is concerned, Eulerian plus Lagrangian approaches were selected to represent the dispersion near the source.

The emissions of three stacks (point sources) were used for the simulation, with the same characteristics as in numerical model, while tracer mode (TR1) was selected for PM_{10} simulation. Figure 2a shows the four grid domains that were used for the TAPM simulation.

2.3 The CFD model (ANSYS-CFX)

ANYS model is a commercial computational fluid dynamics software that is based on the governing fluid flow, the three momentum Reynolds Averaged Navier-Stokes equations and traditional transport equations. The model included condensation and evaporation of the water phase to enable assessment of plume visibility, as well as pollutants dispersion. The following assumptions were made [11]:

- Turbulence was modeled using k-ε approach with buoyancy correction term included, buoyancy flux enhancement factor= 1 (a value of 1 means no enhancement of the standard buoyancy flux).
- The air and vapor behave as ideal gases and the liquid can be regarded as incompressible.
- The latent heat of vaporization is constant over the temperature range considered.

Taking into account the above hypothesis, an ANSYS configuration was made by creating the simulation domain of 500m in each direction. The atmospheric boundary layer conditions were provided by TAPM. ANSYS-CFX was chosen among other software because it is considered to estimate the atmospheric boundary layer more accurately [9]. The whole domain was devised into regions namely: domain inlet, domain outlet, domain top, domain right and left and domain ground, where the three stacks (PS1,PS2 and PS3) were build and considered them to be as point sources in order to simulate PM_{10} dispersion (Figure 2a,). The number of fine grid elements is 2.780.437 for the whole domain. The stacks characteristics are represented in Table 1.

TABLE 1- Characteristics of the three stacks that were used for the simulation.

	PS1	PS2	PS3
Height (m)	115	115	150
Diameter (m)	7.2	7.2	9.3
Exit Velocity (m/s)	15.3	15.3	15.2
Exit Temperature (K)	495	495	495

For the numerical model, three different cases- hours during the episode were selected in order to represent the plume behaviour. The data inputs for the numerical model are average hourly values from the closest measurement station (steady state) and they are illustrated below.

1. At 10:00 UTC, with initial conditions (inlet) 2.3m/s for the wind speed and for temperature 288.2 K.
2. At 14:00 UTC, with initial conditions (inlet) 1.5m/s for the wind speed and for temperature 292.5K.
3. At 20:00 UTC, with initial conditions (inlet) 2.8m/s for wind speed and 287.1K for temperature.

TAPM simulations cover a much larger area of land, and larger grids/mesh elements are used than in CFD modeling described in this paper. Furthermore, TAPM simulations are transient, which means that simulations are being conducted for pollutants dispersion over periods/time. On the other hand, the CFD modeling presented here is a steady state and actually presents a snap-shot of the plumes behavior, with parameters such as emission rates, wind speed and direction to be held constant.

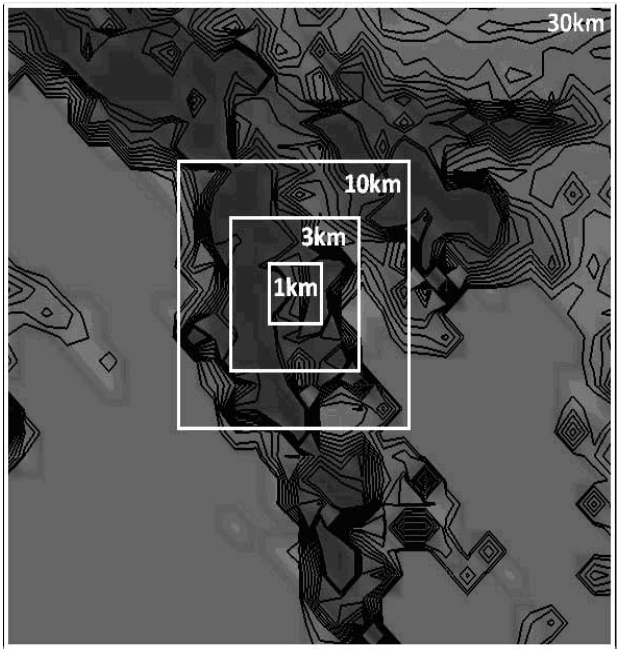

FIGURE 2a – Grid domains used for the TAPM simulation.

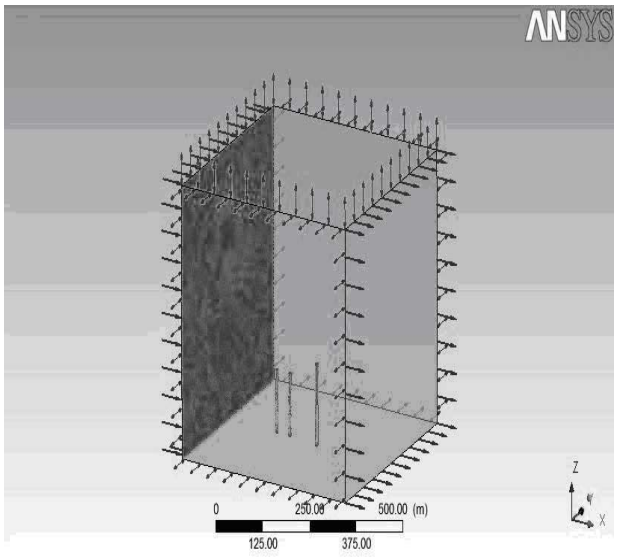

FIGURE 2b – Grid domain created in ANSYS. The colored black side is the domain inlet.

3. RESULTS AND DISCUSSION

3.1 Meteorology Modeling

The vertical profile of potential temperature was calculated by TAPM, as it can be seen in Figure 3, in order to examine the diurnal variation of temperature during the different hours of the day, in conjunction, the average vertical wind profile is also calculated and presented in Figure 5.

As it is evident from the temperatures' variation profile, at 6:00 a strong inversion layer with strength of 4K/300m is evident to extent up to a height of 300m. At 10:00, two hours after the local sunrise, a stable layer with an intense surface based inversion beneath 100m occurs. From the corresponding wind data, a weak easterly flow appears at the surface, while above 100m a westerly direction wind is evident.

Two hours later, at the midday, a deep super adiabatic layer is calculated by TAPM near the ground, and at the same time a weak elevated inversion is existing from 200m to 250m, while at an altitude of 380m and higher, a less stable layer is evident for the same hour. The calculated winds for this hour show a weak north flow from the surface up to 800m with scalar increased intensity. Furthermore, during the warm hours, and specifically at 14:00, a relatively rapidly development of a shallow surface-based convective boundary layer and a height inversion between 250m and 580m is evident, while up to 600m a less stable layer occurs for the same hour. Within the unstable layer an upslope northeast (NE) flow prevailed due to heating of the valley sides. In the stable layer at the same time, the weak winds blow from northwest (NW) to west (W) direction. Two hours later at 16:00 the convective boundary layer is evident at an altitude below 200m, while simultaneously neutral conditions occur between 200m and 400m, probably due to further heating of the valley. Turnings in wind direction below 200m as well as calms are presented in this hour. The formation of that layer, together with the prevailing conditions in the atmosphere in those warm hours, favor the entrapment of pollutants in the lower levels near to the surface, a fact that leads to relatively high ground concentrations.

Two hours after sunset, at 19:00, an inversion layer was created up to 450m. However, within this stable layer a more intense surface-based inversion layer is depicted for the first 180m. Slope winds from west direction resulted from radiative cooling of the valley slopes, assisted the valley floor in filling it with cold air, a situation which created a stable layer of cold air. Moreover, at 21:00, the ground-based inversion reached the 200m and, simultaneously, higher up, a stable less layer is formed.

It should be mentioned that the calculated characteristics of vertical temperature profiles are in agreement with the observations made by experiment through a tethered balloon system in the valley in 1995 [5].

The average daily evolution of the atmospheric boundary layer for 2/12 and 3/12/11 is described in Figure 4. In this Figure the variation of the potential temperature at different heights from 10m to 750m at the center grid of the simulation during the day is illustrated. As it is represented, the potential temperature changes more quickly at lower altitudes as well as during sunrise and sunset periods.

To sum up, the absence of strong synoptic winds at higher levels (4m/s) and the calms that occur beneath 200m and near the surface (0.2- 1m/s) are the main characteristics that favor the development of that shallow convective boundary layer and, consequently, the entrapment of concentrations. Especially at 14:00, opposite vertical

winds from NE (below 50m) to NW direction (above 200m) by the growing convective boundary layer probably caused more unsteadiness [12]. A fact that is also evident in Figure 6, where the zoom of the first 800m is depicted. In those profiles, it is obvious that during the warm hours there is irregularity of direction near the surface until 200m, but above 200m there are no observations of systematic turnings of direction with height. On the other hand, the wind speed profile follows a different pattern. Below 200m and near the surface the wind speed is remaining almost unchanged, with low strength from 0.3m/s to 0.6m/s, while above 200m the strength is changing drastically with height. This behavior of both variables verifies the characteristics of a shallow convective boundary layer.

3.2 PM_{10} Dispersion Modeling

In order to investigate the dispersion from the shortest in height stacks in the region, average mean hourly concentrations of PM_{10} from 2-3/12/11 at the center grid are illustrated in Figure 7a, 7b, 7c, as it were calculated by

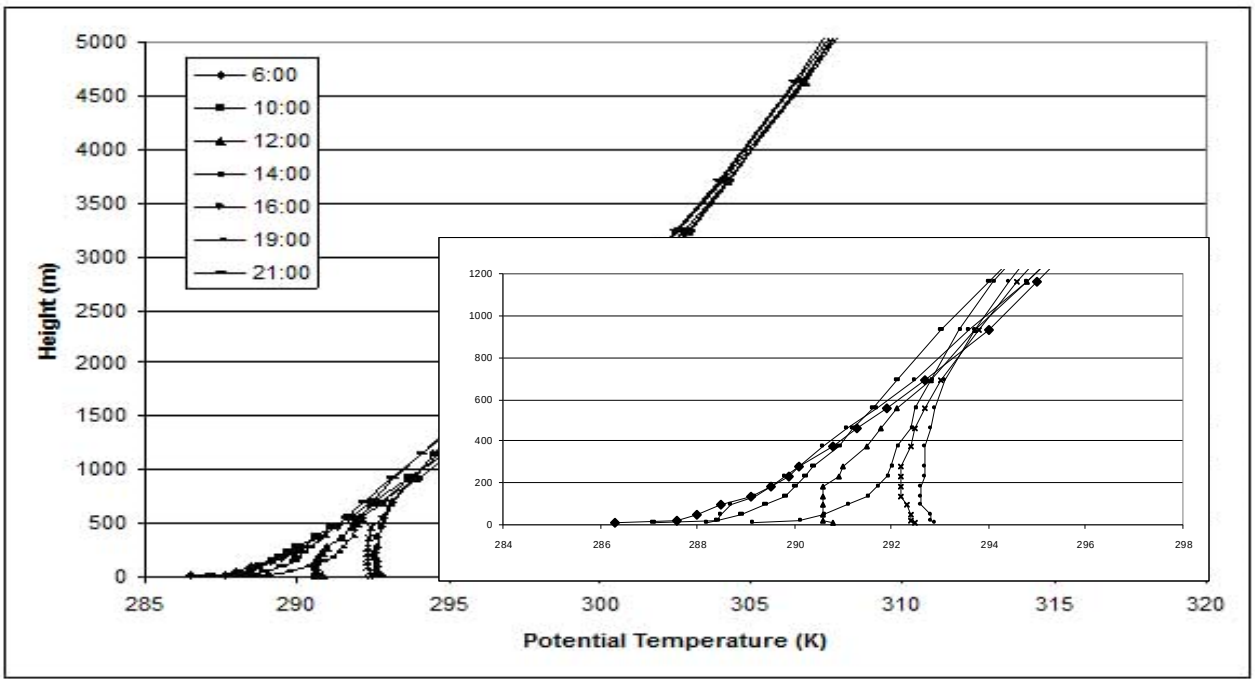

FIGURE 3 – Average vertical profile of Potential Temperature at the center grid point of the simulation, for selected hours during the day, as it was calculated by TAPM. To the right is the zoom for the first 1400m

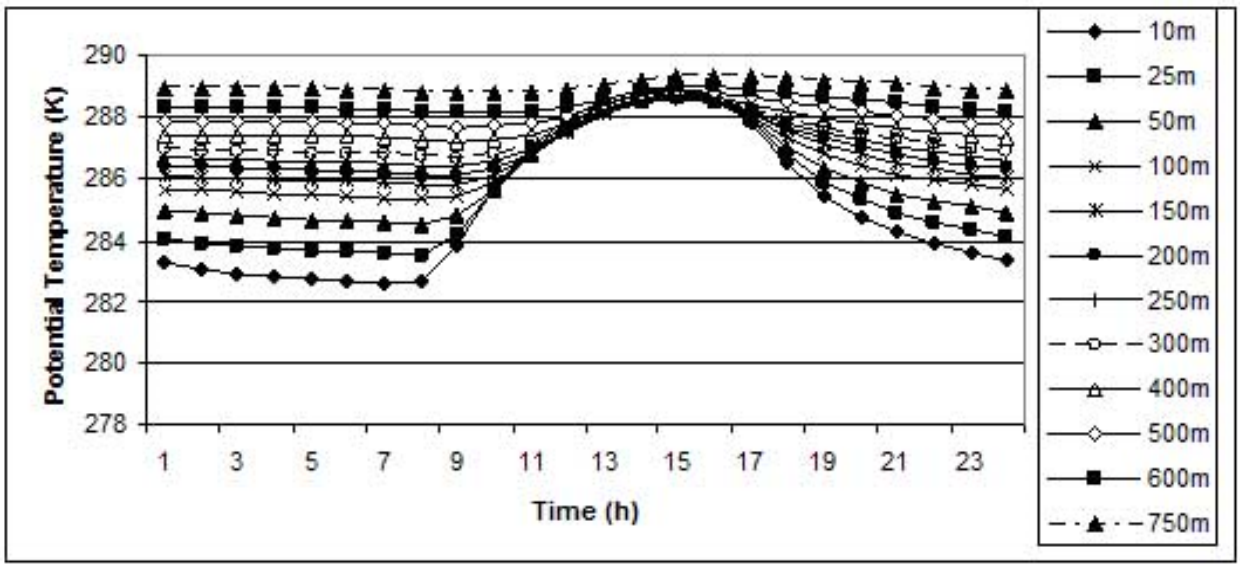

FIGURE 4 – Potential Temperature variation at different heights at the center grid point of the simulation.

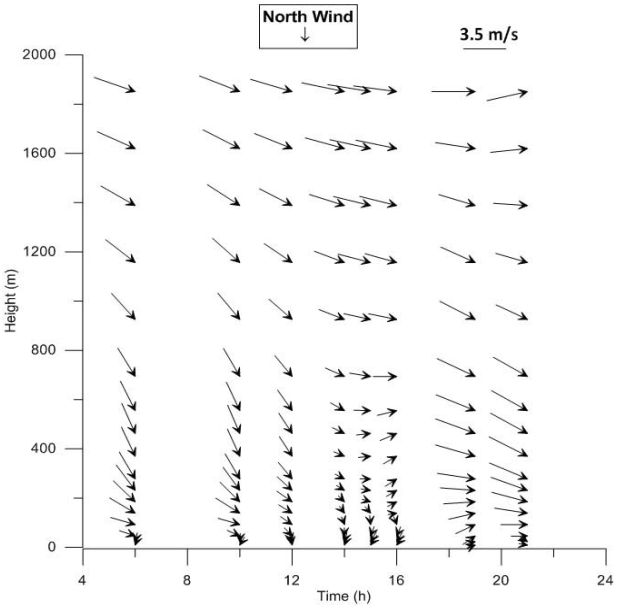

FIGURE 5 – Vertical velocity profile. The vertical winds are at 06:00, 10:00, 12:00, 14:00, 15:00, 16:00, 19:00 and 21:00.

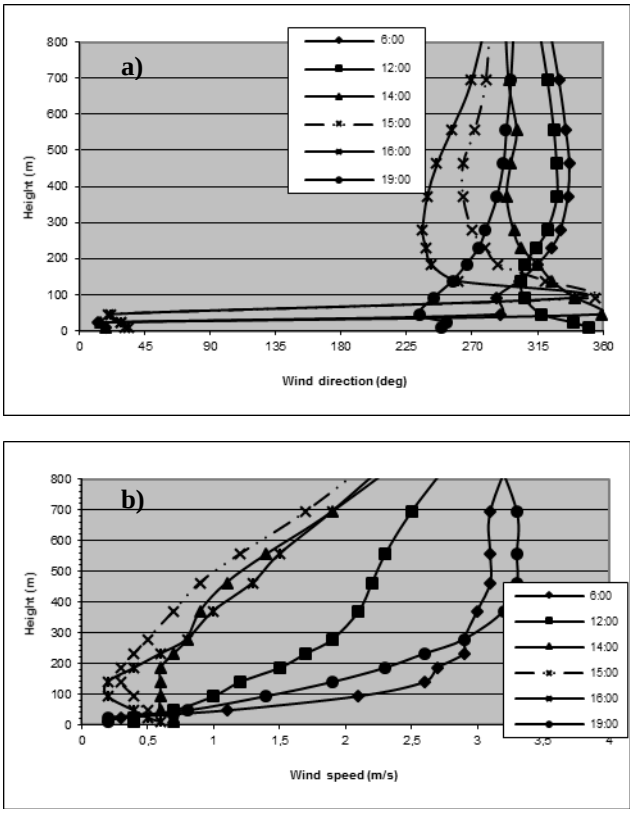

FIGURE 6 – a) Vertical direction profile. b) Vertical speed profile at 06:00, 12:00, 14:00, 15:00, 16:00 and 19:00.

TAPM for the period of morning, noon and night. The behavior of the plume indicates the entrapment of PM_{10} within a stable layer in a fanning form that occurs after sunset, from the early afternoon 17:00 am, until sunrise and late morning 11:00 pm, in the levels of 200m to 400m. Throughout warm hours of the day 12:00 to 16:00 the plume rises up to 800m.

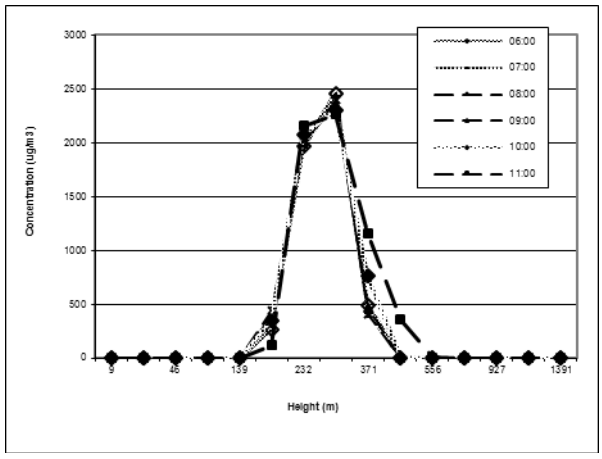

FIGURE 7a–Vertical concentrations of PM_{10} during morning hours.

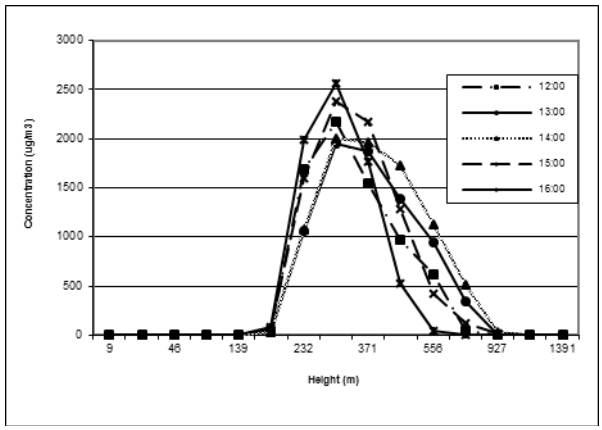

FIGURE 7b –Vertical concentrations of PM_{10} during noon hours.

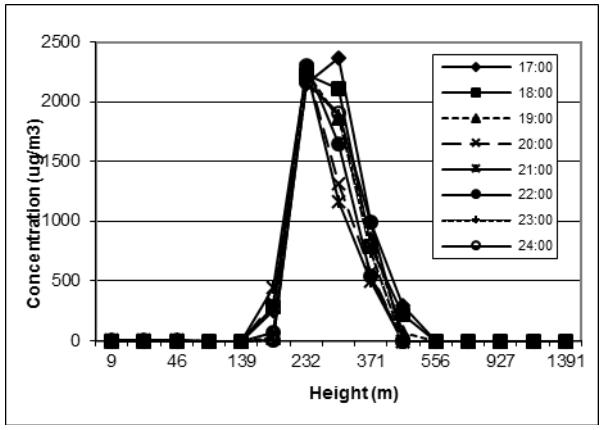

FIGURE 7c –Vertical concentrations of PM_{10} during afternoon and night hours.

The ANSYS model in a steady state mode represented the plumes' behavior at selected hours 10:00pm, 14:00am and 20:00am. A correlation to the numerical model CFD was made with TAPM model and vertical concentration profiles were calculated in contrast to those calculated by TAPM. Figure 8 is showing the vertical PM_{10} concentrations, as it was calculated by ANSYS and TAPM.

The results are in good agreement, with Pearson correlation coefficient to be 0.94, 0.80 and 0.96 for the three

cases where the numerical model was used. Furthermore, from this Figure it appears that both models seem to calculate the entrapment of PM_{10} concentrations in the levels of 200m to 400m. In addition, the plumes' behavior for the three cases, as it is presented by ANSYS and TAPM though daytime, is illustrated in Figure 9. From this Figure it is rather obvious that the dispersion conditions are almost the same during morning and evening hours by both models, while in the warm hours of the day the dispersion changes due to the convective boundary layer as well as solar radiation. More detailed, at 10:00 two hours after sunrise the plume behavior indicates a fanning plume, which is imbedded within a stable inversion layer (Figure 9d). At 14:00 a trapped plume occurs due to the inversion aloft and thus upward dispersion is blocked by the inversion layer above the growing convective layer (Figure 9e). At 20:00 almost the same atmospheric conditions exist, as in the morning case, with the plume behavior to be in a fanning form (Figure 9f).

Average contour plot of the plume in the region was also calculated by TAPM at ground level, in order to see in which grid point of the whole domain the maximum concentration is observed.

The geographical axis of the area in addition to vertical velocity profile, indicate that the prevailing winds were mostly blowing in the northwest direction thus the maximum concentrations observed in that direction. Figure 10 illustrates the average concentration of the simulation as it was calculated by TAPM. Additionally, the average vertical profile of PM_{10} concentrations is also calculated by TAPM for that grid point where the maximum concentration can be seen, during separate hours of the day to investigate the ground concentrations. As it is noticeable the maximum ground concentrations are spotted in the warm hours of the simulation period and more distinctively between 14:00 and 16:00.

The meteorological analysis above, showed that the formation of a surface-based convective boundary layer at an altitude of 200m and a height inversion above were transpired for the same hours, substantiate that the pollutants were trapped in the lower levels and as a result relatively high ground concentrations were observed. The emitted fanning plume is broken up by the rising turbulence, when day –time heating of the ground breaks up the inversion, resulting into trapped and fumigation plumes' behavior.

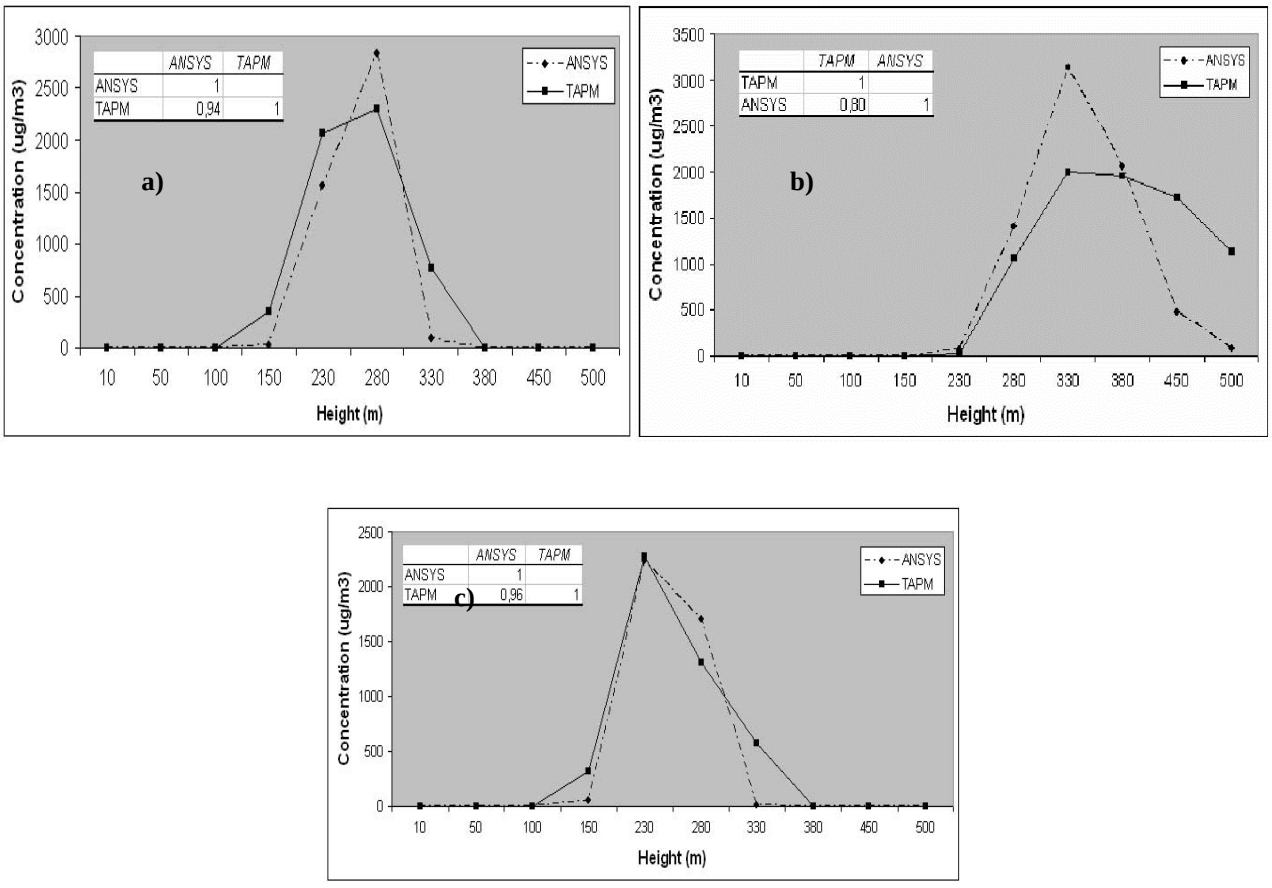

FIGURE 8 –Vertical profile of PM_{10} concentrations as was calculated by ANSYS and TAPM. a) at 10:00 b) at 14:00 c) at 20:00

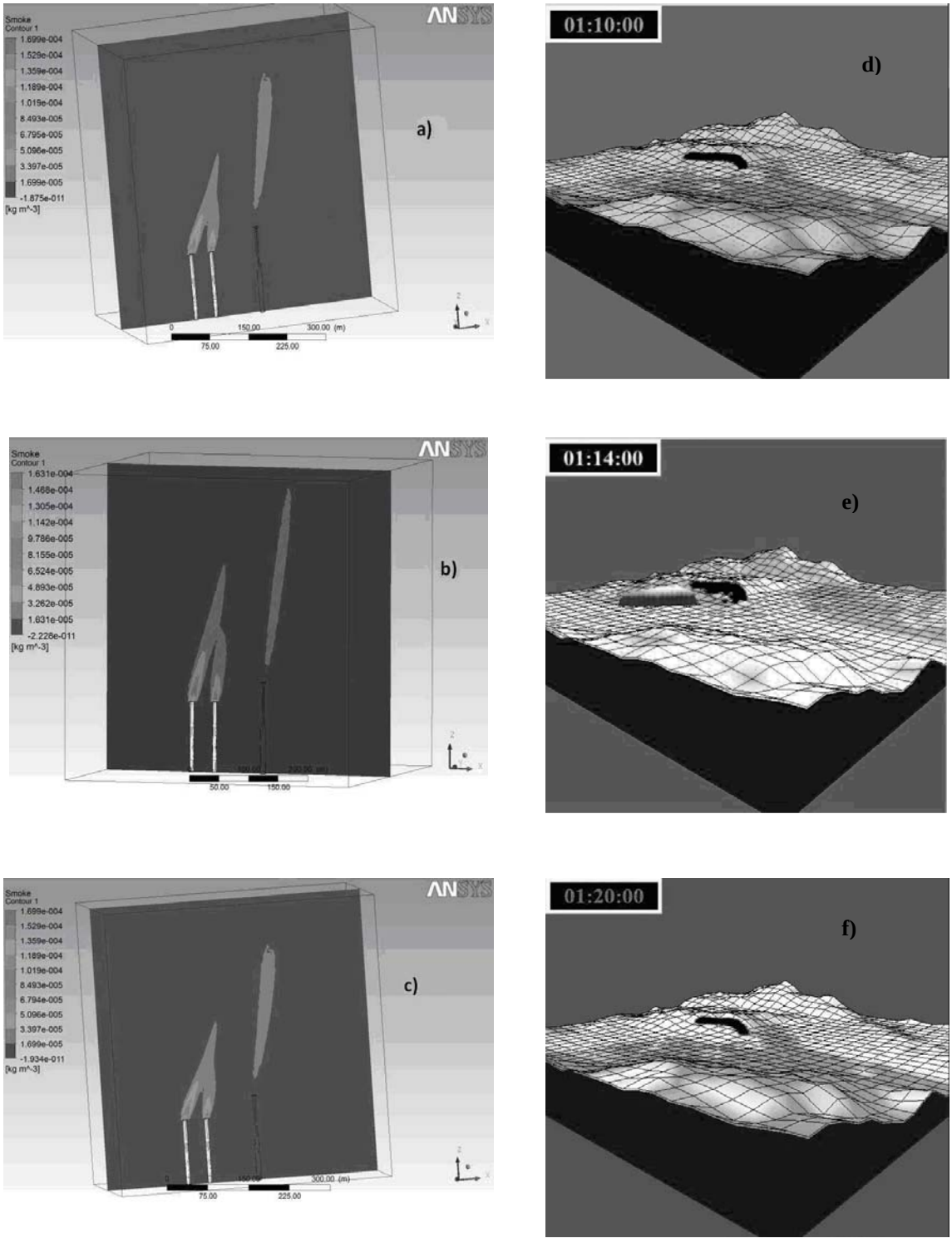

FIGURE 9 –Plumes' behavior calculated by ANSYS and TAPM during daytime simulation. Right images a) to c) are represented by the ANSYS model. Left images e) to f) are represented by the TAPM model.

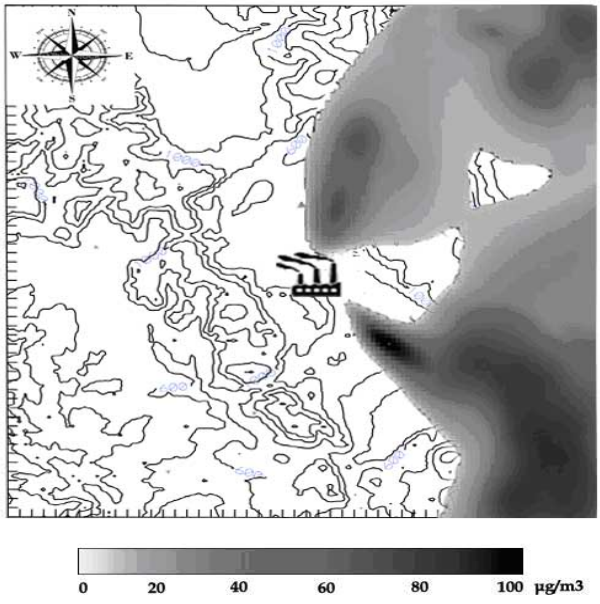

FIGURE 10a –Average contour plot of the plume for 2-3/12/11. Inner grid of the simulation. Elevations are in meters.

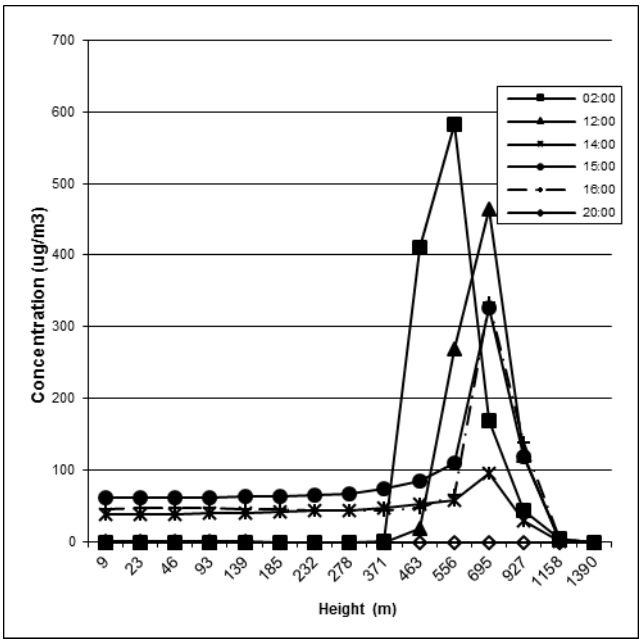

FIGURE 10b –Average vertical profile of PM_{10} concentrations at the maximum concentration grid point for separate hours of daytime.

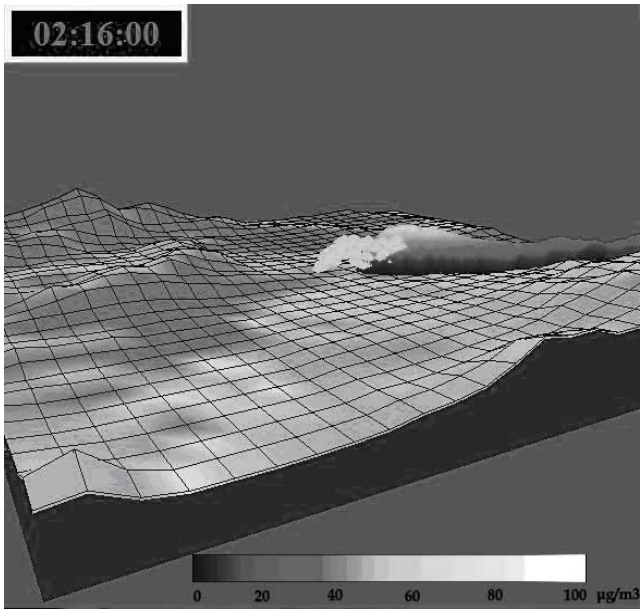

FIGURE 11 –3D plume visualization calculated by TAPM for 3/12/11 at 16:00.

The 3D visualization of the plume is represented in Figure 11. From this Figure below, the curve that applies in plumes' dispersion at 16:00 supports the entrapment of PM_{10} concentrations due to the existence of a shallow convective boundary layer and the height inversion aloft. The entrapment occurs when the plume reaches the inversion height , then retains sufficient buoyancy to resist downward motions and becomes temporally trapped in the lower part of the overlying inversion layer. The PM_{10} concentrations that escaped the influence of the convective boundary layer turbulence, act as a continuous source and they slowly re-enter the convective boundary layer in the process of fumigation [20,21].

4. CONCLUSIONS

The dispersion of pollutants from point sources for an episode case was studied with a microscale and a mesoscale model.

Basic meteorological parameters of the region were analyzed with the implementation of a prognostic meteorological and air pollution model, TAPM.

Temperature inversions in conjunction with vertical profile in winds showed the unsteadiness in the atmosphere and as a consequence the verification of trapped PM_{10} concentration.

The development of a shallow surface-based convective boundary layer is evident during noon hours of the simulation at an altitude below 200m, which reveals the unsteadiness in the atmosphere, and as a result relatively high ground concentrations might appear.

The highest ground level concentrations were calculated at the midday, when the development of the convective layer below 200m and the creation of a height inversion at an altitude above 250m from the ground were occurred.

ANSYS and TAPM models showed the entrapment of PM_{10} concentrations for the levels of 200m to 400m during late morning and late afternoon of the simulation.

Model performance statistics of ANSYS and TAPM showed good correlation 0.94, 0.80 and 0.96 for the three cases that the numerical model was used.

In conclusion, the simulations from both models interpret the mechanism that favors the accumulation of pollutants in the lower levels of the atmosphere. It should be noted that further validation of the modeling results at ground level through a comparison with measurements by the monitoring stations constitutes a subject of future study.

ACKNOWLEDGEMENTS

The authors would like to thank the Greek Public Power Corporation for providing meteorological data from the 10 peripheral stations in the area.

The authors have declared no conflict of interest.

REFERENCES

[1] J.S. Anagnostopoulos, G. Bergeles (1998) A numerical model for wind field and pollutant concentration calculations over complex terrain. Application to Athens, Greece. Wind Engineering and Industrial Aerodynamics 73, 285-306.

[2] S.A. Silvester, I.S. Lowndes, D.M. Hargreaves (2009) A computational study of particulate emissions from an open pit quarry under neutral atmospheric conditions. Atmospheric Environment 43, 6415-6424.

[3] J.A. Torano, R. Rodriguez, I. Diego, J.M. Rivas, A.Pelegry (2007) Influence of pile shape on wind erosion CFD ermission simulation. Applied Mathematical Modelling 31, 2487-2502.

[4] A.F. Karagiannidis, A.G. Triantafyllou, T.S. Karacostas (2013) Analyzing the basic meteorological aspects of a particulate air pollution episode over the industrial area of Northwestern Greece during the November of 2009. Global NEST Journal, vol 15 No2, 241-253.

[5] A.G Triantafyllou, C.G. Helmis, D.N Asimakopoulos and A.T Soilemes (1995), Boundary layer evolution over large and broad mountain basin, Theoritical and Applied Climatology Vol.52, 19-25.

[6] A.G Triantafyllou (2001), PM10 pollution episodes as a funtion of synoptic climatology in a mountainous industrial area, Environmental Pollution Vol. 112/3,491-500.

[7] M. Astitha, G. Kallos, P. Katsafados (2008), Air pollution modeling in the Mediterranean Region: Analysis and forecasting of episodes, Atmospheric Research 89, 358-364.

[8] Jaakko Kukkonen, , Mia Pohjola, Ranjeet S Sokhi, Lakhu Luhana, Nutthida Kitwiroon, Lia Fragkou, Minna Rantamaki, Erik Berge, Viel Ødegaard, Leiv Havard Slørdal, Bruce Denby, Sandro Finardi (2005) Analysis and evaluation of selected local scale PM10 air pollution episodes in four European cities: Helsinki, London, Milan and Oslo, Atmospheric Environment 39, 2759-2773.

[9] B. Blocken, T. Stathopoulos, J. Carmeliet (2007), CFD simulation of the atmospheric boundary layer : wall function problems, Atmospheric Environment 41, 238-252.

[10] Triantafyllou, A.G. and Kassomenos, P. (2003). Aspects of atmospheric flow and dispersion of air pollutants in a mountainous basin, The Science of the Total Environment, 297, 85-103.

[11] G.J Brown and D.F. Fletcher (2005) CFD Prediction of odour dispersion and plume visibility for alumina refinery calciner stacks, Process Safety and Environmental Protection - PROCESS SAF ENVIRON PROT 01/2005; 83(3):231-241. DOI:10.1205/psep.04007

[12] G.A. Briggs (1993), Plume dispersion in the convective boundary layer. Part II: analyses of CONDORS field experiment data. Journal of Applied Meteorology 32, 1388-1425.

[13] Hurley P, Physick W, Luhar A (2005) TAPM—A practical approach to prognostic meteorological and air pollution modeling. Environ Modell & Software 20:737–752.

[14] Luhar A, Hurley P (2003) Evaluation of TAPM, a prognostic meteorological and air pollution model, using urban and rural point-source data. Atmos Environ 37: 2795-2810

[15] A. K. Luhar and P. J. Hurley (2004) Application of a prognostic model TAPM to sea-breaze flows, surface concentrations and fumigating plumes. Environmental Modelling & Software 19, 591-601.

[16] V. Matthaios, A.G. Triantafyllou, T. Albanis (2013) Performance and verification of a downscaling approach for meteorology and land use, using a mesoscale model in a complex terrain industrial area in Greece, Proceedings of the 13th International Conference on Environmental Science and Technology, 5-7 September 2013 Athens, Greece, ISBN 978-960-7475-51-0.

[17] Venkatram A. and Vet R. (1981) Modeling of dispersion from tall stacks. Atmospheric Environment 15, 1531-1538.

[18] Willis G. E. and Deardorff J. W. (1983) On plume rise within a convective boundary layer. Atmospheric Environment 17, 2435-2447.

[19] Technical report for the municipality of Kozani for 2010-2011, November 2011.

[20] Willis G. E. and Deardorff J. W. (1987) Buoyant plume dispersion and inversion entrapment in and above a laboratory mixed layer. Atmospheric Environment 21, 1725-1735.

[21] Ashok K. Luhar and Rex E. Britter (1991) Random-walk modeling of buoyant-plume dispersion in the convective boundary layer. Atmospheric Environment Vol 26A, No7, 1283-1298.

Received: June 04, 2014
Accepted: June 04, 2014

CORRESPONDING AUTHOR

Vasileios. N. Matthaios
Laboratory of Atmospheric Pollution
and Environmental Physics
Dept. of Environmental Engineering
Technological Education Institute (TEI)
of West Macedonia
50100 Kozani
GREECE

E-mail: vmat@airlab.edu.gr
vmatthaios@gmail.com